Stability and Bifurcation Analysis of the Transverse Vibrations of a Cantilever Pipe Conveying Pulsating Two Phase Flow

A.S. Adegoke[1]*, T.A. Fashanu[2], A.A. Oyediran[1]
(1) Department of Mechanical Engineering, University of Lagos, Nigeria (2) Department of Systems Engineering, University of Lagos, Nigeria
Email: adeshinexx@yahoo.com

Abstract
This work presents analytical and numerical analysis of the stability and bifurcation of a cantilevered pipe conveying pulsating two phase flow. Multiple scale perturbation technique is used to obtain the stationary trivial and nontrivial solutions of its response amplitudes. Clearly, the system exhibits both stable and unstable solutions depending on the detuning of the frequencies. The fixed point of the non trivial solutions of the pipe's dynamics is a saddle node bifurcation. On the other hand, trajectories of the trivial solutions present subcritical pitchfork and supercritical pitchfork bifurcations at the critical points. Numerical simulations are observed to be in agreement with analytical results. Also, a study on the effect of void fraction on the bifurcation points shows that at post-critical mixture velocity, a defining void fraction exists when there is a transition between the subcritical pitchfork bifurcation point and supercritical pitchfork bifurcation.

Keywords: Cantilever pipe, Transverse vibration, Pulsating two-phase flow, Stability, Bifurcation

1. INTRODUCTION

Instability in pipes as induced by the conveyed fluid has been a consistent subject of interest in the field of fluid structure interaction. To date, literature emphasized the dynamics of pipes conveying single phase flow (Gregory and Paidoussis (1966), Paidoussis and Issid (1974), Shilling and Lou (1980), Semler; et al (1994), Ghayesh; et al (2013)). However industrial flows through pipes do not always exist as single phase. Depending on the temperature, pressure and nature of fluid; concurrent flow of two or more phases are conveyed by the pipes. Leveraging on the existing in-depth studies on pipes conveying single phase flow, recent publications have shown that pipes conveying two phase flow exhibits some complex and fascinating dynamics. Monette and Pettigrew (2004); published what might be one of the premier papers on the dynamics of pipes conveying two phase flow. The work used experimental and theoretical techniques to investigate fluid-elastic instability of flexible tubes that are subjected to two-phase flow. It established the relationship between the void fraction and the linear dynamics of the pipe. Also on two phase flows in pipes, Adegoke and Oyediran (2018); linearly studied the effect of temperature, pressure and void fractions on the attainment of the critical velocities via Argand diagrams. Furthermore, Adegoke and Oyediran (2017); studied the nonlinear vibrations of top-tensioned cantilevered pipes using the method of multiple-scale assessment. The work revealed that at some frequencies the system is uncoupled, while at other frequencies a 1:2 coupling exists between the axial and the transverse frequencies of the pipe. Adegoke, et al. (2019); studied the nonlinear coupled parametric resonance of a cantilever pipe conveying pulsating two phase flow with the tendency of both phases pulsating at the same frequency. Wang, et al. (2018); studied the dynamic behaviours of horizontal gas-liquid pipes subjected to hydrodynamic slug flow; modeling and experiments. The work adapted the linear equation of transverse motion for single phase flow to account for the two phases and resolved the modified equation using finite element method. In addition, experiments were performed to measure the characteristic parameters of the hydrodynamic slugs and the dynamics response of the pipe. Chen and Jian (2015); used the generalized integral transform technique to study the effect of

the volumetric quality and the volumetric flow rate on the dynamic behaviour of pipes conveying two phase flows.

In this paper, the stability and bifurcations of a cantilevered pipe conveying pulsating two phase flow is studied using analytical and numerical techniques. The method of multiple scale perturbation is used to establish the parametric resonance relationship. The nature of the bifurcations exhibited by the pipe and the possible effect of variation in void fraction on the bifurcations are examined and the void fraction that precipitated to the transition between the supercritical and subcritical pitchfork bifurcations was investigated.

2. PROBLEM FORMULATION AND MODELLING

2.1. Assumptions

Consider a cantilever cylindrical pipe of length (L), with a cross-sectional area (A), mass per unit length (mp) and flexural rigidity (EI), conveying multiphase flow; the flow is parallel to the pipe's centre line. It is assumed that the velocity profile can be represented as a plug flow. The diameter of the pipe is small compared to its length, such that the pipe behaves like an Euler-Bernoulli beam. The motion is planar. The deflections of the pipe are large, but the strains are small. Rotatory inertia and shear deformation are neglected. Pipe centerline assumed to be extensible.

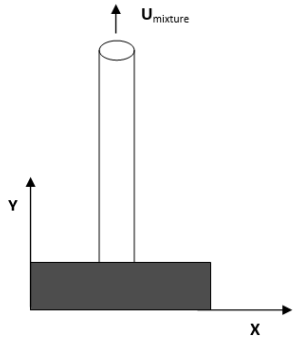

Figure 1: System's Schematics

2.2 Equation of motion of an extensible cantilever pipe conveying multiphase flow

The equations of motion for an extensible cantilever pipe conveying pressurized unsteady multiphase flow under thermal loading as expressed by Adegoke and Oyediran (2018) are presented as:

$$\left(m+\sum_{j=1}^{n}M_j\right)\ddot{u}+\sum_{j=1}^{n}M_j\dot{U}_j+\sum_{j=1}^{n}2M_jU_j\dot{u}'+\sum_{j=1}^{n}M_j{U_j}^2u''+\sum_{j=1}^{n}M_j\dot{U}_ju'-EAu''-EI\left(v''''v'+v''v'''\right)$$
$$+(T_0-P-EA(\alpha\Delta T)-EA)v'v''-\left(T_0-P-EA(\alpha\Delta T)\right)'+\left(m+\sum_{j=1}^{n}M_j\right)g$$
$$=0 \qquad (1)$$

$$\left(m+\sum_{j=1}^{n}M_j\right)\ddot{v}+\sum_{j=1}^{n}2M_jU_j\dot{v}'+\sum_{j=1}^{n}M_j{U_j}^2v''-\sum_{j=1}^{n}aM_j{U_j}^2v''+\sum_{j=1}^{n}M_j\dot{U}_jv'+EIv''''$$
$$-\left(T_0-P-EA(\alpha\Delta T)\right)v''$$
$$-EI\left(3u'''v''+4v'''u''+2u'v''''+v'u''''+2{v'}^2v''''+8v'v''v'''+2{v''}^3\right)$$
$$+\left(T_0-P-EA(\alpha\Delta T)-EA\right)\left(u'v''+v'u''+\frac{3}{2}{v'}^2v''\right)$$
$$=0 \tag{2}$$

The associated boundary conditions for a pipe from end 0 to L are:

$$v(0)=v'(0)\text{ and }v''(L)=v'''(L)=0, \tag{3}$$
$$u(0)=u'(L)=0. \tag{4}$$

2.3 Dimensionless equation of motion for multiphase flow

Neglecting the axial direction, the transverse vibration's equation of motion may be rendered dimensionless by introducing the following non-dimensional quantities;

$$\bar{v}=\frac{v}{L}\ ,\quad \bar{t}=\left[\frac{EI}{\sum M_j+m}\right]^{1/2}\frac{t}{L^2}\ ,$$
$$\bar{\mathbf{U}}_j=\left[\frac{M_j}{EI}\right]^{1/2}UL\ ,\ \gamma=\frac{\sum M_j+m}{EI}L^3g,$$
$$\beta_j=\frac{M_j}{\sum M_j+m},\quad \Psi_j=\frac{M_j}{\sum M_j},\Pi_0=\frac{T_oL^2}{EI}\ ,\ \Pi_1=\frac{EAL^2}{EI},\Pi_2=\frac{PL^2}{EI}.$$

The dimensionless equation can be reduced to that of a two-phase as:

$$\ddot{\bar{v}}+2\bar{\mathbf{U}}_1\sqrt{\Psi_1}\sqrt{\beta_1}\dot{\bar{v}}'+2\bar{\mathbf{U}}_2\sqrt{\Psi_2}\sqrt{\beta_2}\dot{\bar{v}}'+\Psi_1{\overline{\mathbf{U}_1}}^2\bar{v}''+\Psi_2{\overline{\mathbf{U}_2}}^2\bar{v}''-a\Psi_1{\overline{\mathbf{U}_1}}^2\bar{v}''-a\Psi_2{\overline{\mathbf{U}_2}}^2\bar{v}''+$$
$$\dot{\overline{\mathbf{U}_1}}\sqrt{\Psi_1}\sqrt{\beta_1}\bar{v}'+\dot{\overline{\mathbf{U}_2}}\sqrt{\Psi_2}\sqrt{\beta_2}\bar{v}'-\left(\Pi_0-\Pi_2-\Pi_1(\alpha\Delta T)\right)\bar{v}''+\bar{v}''''-\left(2{\bar{v}'}^2\bar{v}''''+8\bar{v}'\bar{v}''\bar{v}'''+\right.$$
$$\left.2{\bar{v}''}^3\right)+\left(\Pi_0-\Pi_2-\Pi_1(\alpha\Delta T)-\Pi_1\right)\left(\frac{3}{2}{\bar{v}'}^2\bar{v}''\right)=0. \tag{5}$$

The dimensionless boundary conditions are:

$$\bar{v}(0)=\bar{v}'(0)\text{ and }\bar{v}''(1)=\bar{v}'''(1)=0, \tag{6}$$

Assuming that the phase velocities are harmonically fluctuating about constant mean velocities,

$$\bar{\mathbf{U}}_1=\bar{U}_1\left(1+\mu_1\sin(\Omega_1T_0)\right), \tag{7}$$
$$\bar{\mathbf{U}}_2=\bar{U}_2\left(1+\mu_2\sin(\Omega_2T_0)\right), \tag{8}$$

Using these notation,

$$C21=2\sqrt{\Psi_1}\sqrt{\beta_1}\ ,\ C22=2\sqrt{\Psi_2}\sqrt{\beta_2}\ ,\ C31=\Psi_1\ \ C32=\Psi_2,\ C5=\Pi_1,\ C6=(\Pi_0-\Pi_2-\Pi_1(\alpha\Delta T)-\Pi_1),\ C7=\Pi_0-\Pi_2-\Pi_1(\alpha\Delta T).$$

Equation (5) can be reduced to:

$$\ddot{\bar{v}} + \overline{\mathbf{U}}_1 C21\dot{\bar{v}}' + \overline{\mathbf{U}}_2 C22\dot{\bar{v}}' + C31\overline{\mathbf{U}_1}^2\bar{v}'' + C32\overline{\mathbf{U}_2}^2\bar{v}'' - aC31\overline{\mathbf{U}_1}^2\bar{v}'' - aC32\overline{\mathbf{U}_2}^2\bar{v}'' + \overline{\dot{\mathbf{U}}_1}\, C11\bar{v}' + \overline{\dot{\mathbf{U}}_2}\, C12\bar{v}' - C7\bar{v}'' + \bar{v}'''' - \left(2\bar{v}'^2\bar{v}'''' + 8\bar{v}'\bar{v}''\bar{v}''' + 2\bar{v}''^3\right) + C6\left(\frac{3}{2}\bar{v}'^2\bar{v}''\right) = 0. \quad (9)$$

3. METHOD OF SOLUTION

Adopting the empirical relationship for a gas-liquid flow by Adegoke and Oyediran (2018), as derived from the Chisholm Equation by Woldesemayat and Ghajar (2007). An approximate solution of the perturbed dimensionless Equations for $\bar{u}$ and $\bar{v}$ is expressed in the form:

$$\ddot{\bar{v}} + \overline{\mathbf{U}}_1 C21\dot{\bar{v}}' + \overline{\mathbf{U}}_2 C22\dot{\bar{v}}' + C31\overline{\mathbf{U}_1}^2\bar{v}'' + C32\overline{\mathbf{U}_2}^2\bar{v}'' - aC31\overline{\mathbf{U}_1}^2\bar{v}'' - aC32\overline{\mathbf{U}_2}^2\bar{v}'' + \overline{\dot{\mathbf{U}}_1}\, C11\bar{v}' + \overline{\dot{\mathbf{U}}_2}\, C12\bar{v}' - C7\bar{v}'' + \bar{v}'''' + \varepsilon\left(-\left(2\bar{v}'^2\bar{v}'''' + 8\bar{v}'\bar{v}''\bar{v}''' + 2\bar{v}''^3\right) + C6\left(\frac{3}{2}\bar{v}'^2\bar{v}''\right)\right) = 0. \quad (10)$$

Also, perturbing the harmonically fluctuating velocities about their mean values $\overline{U_1}$ and $\overline{U_2}$; such that,

$$\overline{\mathbf{U}_1} = \overline{U_1}\,(1 + \varepsilon\mu_1 \sin(\Omega_1 T_0)) \text{ and}$$
$$\overline{\mathbf{U}_2} = \overline{U_2}\,(1 + \varepsilon\mu_2 \sin(\Omega_2 T_0))\,. \quad (11)$$

Where Ω_1 and Ω_2 are the pulsation frequencies. Therefore, an approximate solution for $\bar{u}$ and $\bar{v}$ can be derived in the form:

$$\bar{v} = \bar{v}_0(T_0, T_1) + \varepsilon\bar{v}_1(T_0, T_1) + \varepsilon^2\bar{v}_2(T_0, T_1) + O(\varepsilon). \quad (12)$$

Considering two time scale, $T_0 = t$ and $T_1 = \varepsilon t$. Where ε is a small dimensionless measure of the amplitude of $\bar{u}$ and $\bar{v}$, used as a book-keeping parameter. Based on the foregoing, the time derivatives operators are:

$$\frac{d}{dt} = D_0 + \varepsilon D_1 + \varepsilon^2 D_2 + O(\varepsilon), \quad (13)$$
$$\frac{d^2}{dt^2} = {D_0}^2 + 2\varepsilon D_0 D_1 + \varepsilon^2({D_1}^2 + 2D_0 D_2) + O(\varepsilon), \quad (14)$$
$$\text{Where } D_n = \frac{\partial}{\partial T_n}. \quad (15)$$

Substituting Equations (11), to (14) into Eq. (10) and equating the coefficients of (ε) of order zero and one respectively gives;

$$O(\varepsilon^0). \quad {D_0}^2\bar{v}_0 - C7\bar{v}_0'' + \bar{v}_0'''' + C21D_0\bar{v}_0'\overline{U}_1 + C22D_0\bar{v}_0'\overline{U}_2 + C31\bar{v}_0''{\overline{U}_1}^2 + C32\bar{v}_0''{\overline{U}_2}^2 - aC31\bar{v}_0''{\overline{U}_1}^2 - aC32\bar{v}_0''{\overline{U}_2}^2 = 0, \quad (16)$$

$$O(\varepsilon^1). \quad {D_0}^2\bar{v}_1 - C7\bar{v}_1'' + \bar{v}_1'''' - 3\bar{v}_0''\bar{v}_0''' - 2{\bar{v}_0'''}^2 - 2\bar{v}_0''''\bar{v}_0'^2 + 2D_0D_1\bar{v}_0 + C31\bar{v}_1''{\overline{U}_1}^2 + C32\bar{v}_1''{\overline{U}_2}^2 - 8\bar{v}_0'\bar{v}_0''\bar{v}_0''' + \frac{3}{2}C6\bar{v}_0'^2\bar{v}_0'' + C21D_0\bar{v}_0'\overline{U}_1 + C22D_0\bar{v}_0'\overline{U}_2 + C21D_1\bar{v}_0'\overline{U}_1 + C22D_1\bar{v}_0'\overline{U}_2 - aC31\bar{v}_1''{\overline{U}_1}^2 - aC32\bar{v}_1''{\overline{U}_2}^2 + 2C31\mu_1\sin(\Omega_1T_0){\overline{U}_1}^2\bar{v}_0'' + 2C32\mu_2\sin(\Omega_2T_0){\overline{U}_2}^2\bar{v}_0'' + C21\mu_1\sin(\Omega_1T_0)D_0\overline{U}_1\bar{v}_0' + C22\mu_2\sin(\Omega_2T_0)D_0\overline{U}_2\bar{v}_0' - 2aC31\mu_1\sin(\Omega_1T_0){\overline{U}_1}^2\bar{v}_0'' - 2aC32\mu_2\sin(\Omega_2T_0){\overline{U}_2}^2\bar{v}_0'' + C41\Omega_1\mu_1\cos(\Omega_1T_0)\overline{U}_1\bar{v}_0' + C42\Omega_2\mu_2\cos(\Omega_2T_0)\overline{U}_2\bar{v}_0' = 0. \quad (17)$$

The homogeneous solution of the leading order Equation (16) can be expressed as:

$$\bar{v}(x, T_0, T_1)_0 = \eta(x)_n \exp(i\lambda_n T_0) + CC. \quad (18)$$

Where (CC) is the complex conjugate, and $\eta(x)_n$ is the complex modal functions for transverse vibrations for each mode (n) and, λ_n is the eigenvalues for the transverse vibrations for each mode (n). The natural frequencies can be estimated by solving the quartic Equation (19) and the condition of obtaining a non-trivial solution of the boundary condition matrix (21) simultaneously.

$$z^4{}_{jn} + \left(C7 - C31\bar{U}_1{}^2 - C32\bar{U}_2{}^2 + aC31\bar{U}_1{}^2 + aC32\bar{U}_2{}^2\right) z^2{}_{jn} - (C21\bar{U}_1 + C22\bar{U}_2) z_{jn}\lambda_n - \lambda^2{}_n = 0, \quad j = 1,2,3,4 \text{ and } n = 1,2,3,4,5 \ldots \quad (19)$$

Boundary condition matrix:

$$\underbrace{\begin{bmatrix} 1 & 1 & 1 & 1 \\ z_{1n} & z_{2n} & z_{3n} & z_{4n} \\ (z_{1n})^2.\exp(i.z_{1n}) & (z_{2n})^2.\exp(i.z_{2n}) & (z_{3n})^2.\exp(i.z_{3n}) & (z_{4n})^2.\exp(i.z_{4n}) \\ (z_{1n})^3.\exp(i.z_{1n}) & (z_{2n})^3.\exp(i.z_{2n}) & (z_{3n})^3.\exp(i.z_{3n}) & (z_{4n})^3.\exp(i.z_{4n}) \end{bmatrix}}_{G} \cdot \begin{bmatrix} 1 \\ H2_n \\ H3_n \\ H4_n \end{bmatrix} . H1_n = \begin{pmatrix} 0 \\ 0 \\ 0 \\ 0 \end{pmatrix} \quad (20)$$

For a non-trivial solution, the determinant of (G) must varnish, That is:

$$DET(G) = 0. \quad (21)$$

Where (λ_n), are the natural frequencies and (Z_n) are the eigenvalues. The mode function of the transverse vibration corresponding to the nth eigenvalue is expressed as:

$$\eta(x)_n = H1_n.\left[e^{x.z_{1n}.i} - (A + B + C + D) - E\right]. \quad (22)$$

Where:

$$A = \frac{e^{x.z_{4n}.i}.\ [e^{z_{1n}.i}.(z_{1n})^3.z_{2n} - e^{z_{1n}.i}.(z_{1n})^3.\ z_{3n} - e^{z_{1n}.i}.\ z_{4n}.(z_{1n})^2.z_{2n}}{(z_{2n} - z_{4n}).(z_{3n} - z_{4n}).[e^{z_{2n}.i}.(z_{2n})^2 - e^{z_{3n}.i}.(z_{3n})^2]},$$

$$B = \frac{e^{x.z_{4n}.i}.\ [e^{z_{1n}.i}.z_{4n}.(z_{1n})^2.z_{3n} - e^{z_{2n}.i}.z_{1n}.(z_{2n})^3 + e^{z_{2n}.i}.\ z_{4n}.z_{1n}.(z_{2n})^2}{(z_{2n} - z_{4n}).(z_{3n} - z_{4n}).[e^{z_{2n}.i}.(z_{2n})^2 - e^{z_{3n}.i}.(z_{3n})^2]},$$

$$C = \frac{e^{x.z_{4n}.i}.\ [e^{z_3.i}.z_{1n}.(z_{3n})^3 - e^{z_3.i}.z_{4n}.z_{1n}.(z_{3n})^2 + e^{z_{2n}.i}.(z_{2n})^3.z_{3n}}{(z_{2n} - z_{4n}).(z_{3n} - z_{4n}).[e^{z_{2n}.i}.(z_{2n})^2 - e^{z_{3n}.i}.(z_{3n})^2]},$$

$$D = \frac{e^{x.z_{4n}.i}.\ [-e^{z_{2n}.i}.z_{4n}.(z_{2n})^2.z_{3n} - e^{z_3.i}.z_{2n}.(z_{3n})^3 + e^{z_3.i}.z_{4n}.z_{2n}.(z_{3n})^2}{(z_{2n} - z_{4n}).(z_{3n} - z_{4n}).[e^{z_{2n}.i}.(z_{2n})^2 - e^{z_{3n}.i}.(z_{3n})^2]},$$

$$E = \frac{e^{x.z_{2n}.i}.(z_{1n} - z_{4n}).[e^{z_1.i}.\ (z_{1n})^2 - e^{z_3.i}.(z_{3n})^2]}{(z_{2n} - z_{4n}).\ [e^{z_2.i}.(z_{2n})^2 - e^{z_3.i}.(z_{3n})^2]} + \frac{e^{x.z_3.i}.(z_{1n} - z_{4n}).[e^{z_{1n}.i}.\ (z_{1n})^2 - e^{z_2 i}.(z_{2n})^2]}{(z_{3n} - z_{4n}).\ [e^{z_2.i}.(z_{2n})^2 - e^{z_3.i}.(z_{3n})^2]}.$$

3.1. Principal parametric resonance

Substituting Equation (18) into the Equation (17) gives;

$$D_0{}^2\bar{v}_1 - C7\bar{v}_1{}'' + \bar{v}_1{}'''' + C21D_0\bar{v}_1{}'\bar{U}_1 + C22D_0\bar{v}_1{}'\bar{U}_2 + C31\bar{v}_1{}''\bar{U}_1{}^2 + C32\bar{v}_1{}''\bar{U}_2{}^2 - aC31\bar{v}_1{}''\bar{U}_1{}^2 - aC32\bar{v}_1{}''\bar{U}_2{}^2 = \left(-B1\left[\frac{\partial Y(T_1)}{\partial T_1}\right] + B2\left[Y(T_1)^2\overline{Y(T_1)}\right]\right)\exp(i\lambda T_0) + \left[B3\left[\exp(-i\Omega_2 T_0) - \exp(i\Omega_2 T_0)\right] + B4\left[\exp(-i\Omega_1 T_0) - \exp(i\Omega_1 T_0)\right]\right]Y(T_1)\exp(i\lambda T_0) + \left[B5\left[\exp(-i\Omega_2 T_0) - \exp(i\Omega_2 T_0)\right] + B6\left[\exp(-i\Omega_1 T_0) - \exp(i\Omega_1 T_0)\right]\right]\overline{Y(T_1)}\exp(-i\lambda T_0) + NST. \quad (23)$$

Here NST denote non-secular terms. The proximity of the nearness can be expressed as:

$$\Omega 1 = 2\lambda + \varepsilon\sigma_2 \text{ and } \Omega 2 = 2\lambda + \varepsilon\sigma_2, \quad (24)$$

Where σ_2 is the detuning parameter. Substituting the Equations of nearness to resonance Equation (24) into Equation (23) and replacing εT_0 with T_1. The secular terms are collated as:

$$\left(-B1\left[\frac{\partial Y(T_1)}{\partial T_1}\right] + B2\left[Y(T_1)^2\overline{Y(T_1)}\right]\right)\exp(i\lambda T_0) + \left[[B7 + B8]\exp(i\varepsilon\sigma_2 T_0)\right]\overline{Y(T_1)}\exp(i\lambda T_0) = 0. \quad (25)$$

The solvability condition demands that the coefficient of $\exp(i\lambda T_0)$ should vanish; Nayfeh (2004), Nayfeh and Mook (1995), Thomsen (2003). This implies that, Y (T_1) should satisfy the following relation:

$$-B1\left[\frac{\partial Y(T_1)}{\partial T_1}\right] + B2\left[Y(T_1)^2\overline{Y(T_1)}\right] + \left[[B7 + B8]\exp(i\varepsilon\sigma_2 T_0)\right]\overline{Y(T_1)} = 0. \quad (26)$$

With the inner product defined for complex functions on [0, 1] as:

$$\langle f, g\rangle = \int_0^1 f\bar{g}\,dx. \quad (27)$$

Equation (26) can be cast as:

$$\frac{\partial Y(T_1)}{\partial T_1} + NY(T_1)^2\overline{Y(T_1)} + M\overline{Y(T_1)}\exp(i\sigma_2 T_1) = 0 \quad (28)$$

Where: $N = \frac{\int_0^1 [B2]\overline{\eta(x)}dx}{-\int_0^1 [B1]\overline{\eta(x)}dx}$, $M = \frac{\int_0^1 [B7+B8]\overline{\eta(x)}dx}{-\int_0^1 [B1]\overline{\eta(x)}dx}$.

To determine $Y(T_1)$, the solution of Equation (28) is expressed in polar form as:

$$Y(T_1) = \frac{1}{2}\alpha y(T_1)e^{i\beta y(T_1)},\ \overline{Y(T_1)} = \frac{1}{2}\alpha y(T_1)e^{-i\beta y(T_1)}. \quad (29)$$

Substituting into the solvability condition and separating real and imaginary parts. The following set of modulation equation is formed:

$$0 = \frac{d\alpha y(T_1)}{dT_1} + \frac{SR\alpha y(T_1)^3}{4} + MR\alpha y(T_1)\cos(\psi) - MI\alpha y(T_1)\sin(\psi), \quad (30)$$

$$0 = \alpha y(T_1)\frac{d\beta y(T_1)}{dT_1} + \frac{SI\alpha y(T_1)^3}{4} + MR\alpha y(T_1)\sin(\psi) + MI\alpha y(T_1)\cos(\psi). \quad (31)$$

Where: $= \sigma_2 T_1 - 2\beta y(T_1)$,

NR and MR are the real part of N and M,
NI and MI are the imaginary part of N and M.

Seeking for stationary solutions, $\alpha(y)' = \psi' = 0$ in modulation Equation (30 and 31)

$$0 = \frac{NR\alpha y(T_1)^2}{4} + MR\cos(\psi) - MI\sin(\psi), \quad (32)$$

$$0 = \frac{\sigma_2}{2} + \frac{NI\alpha y(T_1)^2}{4} + MR\sin(\psi) + MI\cos(\psi). \quad (33)$$

Therefore;

$$\psi = \tan^{-1}\left(\frac{NI\alpha y(T_1)^2 + 2\sigma_2}{NR\alpha y(T_1)^2}\right) - \tan^{-1}\left(\frac{MI}{MR}\right)$$

Such that;

$$(NI^2 + NR^2)\alpha y(T_1)^4 + 4NI\sigma_2\alpha y(T_1)^2 - 16MR^2 - 16MI^2 + 4{\sigma_2}^2 = 0. \quad (34)$$

$$\alpha y(T_1)^2 = 0 \text{ or } \alpha y(T_1)^2 = \frac{-2.NI.\sigma_2}{NI^2+NR^2} \pm \frac{2\sqrt{4.MI^2.NI^2+4.MI^2.NR^2+4.MR^2.NI^2+4.MR^2.NR^2-NR^2{\sigma_2}^2}}{NI^2+NR^2} \quad (35)$$

Therefore, considering the n-th values of $\alpha y(T_1)$ and $\beta y(T_1)$ corresponding to the n-th modal functions and the n-th natural frequencies, the n-th solution of coupled problem is expressed as:

$$\bar{v}(x,t)_n = \alpha y(T_1)_n \eta(x)_n \cos(\lambda_n T_0 + \beta y(T_1)_n) + O(\varepsilon). \quad (36)$$

Substituting into the Equation (36),
$T_0 = t\,, T_1 = \varepsilon t,\ \alpha y(T_1)_n = \alpha y_n,\ \beta y(T_1)_n = \frac{\sigma_{2_n} T_1 - \psi_n}{2},\ \Omega 1 = 2\lambda_n + \varepsilon\sigma_{2_n},\ \Omega 2 = 2\lambda_n + \varepsilon\sigma_{2_n},$
$\Omega 1 = \Omega 2 = \Omega.$

The first order approximate solution is expressed as:

$$\bar{v}(x,t) = \sum_{n=1}^{\infty} \alpha y_n |\eta(x)_n| \cos\left(\frac{(t\Omega - \psi)}{2} + \varphi y_n\right) + O(\varepsilon)\,, \quad (37)$$

Where the phase angles φy_n is given by:

$$\tan(\varphi y_n) = \frac{Im\{\eta(x)_n\}}{Re\{\eta(x)_n\}}. \quad (38)$$

3.2. Stability of fixed points

To characterize the stability of the fixed points and also the various periodic solutions, the Jacobian is derived from Equations (32 and 33) as:

$$J = \begin{bmatrix} -\frac{NR.\alpha y(T_1)}{2} & MI.\cos(\psi) + MR.\sin(\psi) \\ -\frac{NI.\alpha y(T_1)}{2} & MI.\sin(\psi) - MR.\cos(\psi) \end{bmatrix}, \quad (39)$$

The characteristics equation is obtained by solving for the eigenvalues of the Jacobian,

$$|J - \vartheta I| = 0, \text{where } \vartheta \text{ are the eigenvalues.} \quad (40)$$

The problem is characterized by two types of fixed points: Trivial fixed points corresponding to $\alpha y(T_1) = 0$ and nontrivial fixed points corresponding to $\alpha y(T_1) \neq 0$. However, to analyze the stability of the nonlinear solution (nontrivial solution), we substitute the solutions of $\alpha y(T_1)$ as obtained from Equation (35) into the characteristic equation:

$$\vartheta^2 + C1\vartheta + C2 = 0, \quad (41)$$

Where,

$$C1 = MR\cos(\psi) - MI\sin(\psi) + \frac{NR\alpha y(T_1)}{2},$$
$$C2 = \frac{MI.NI.\alpha y(T_1).\cos(\psi)}{2} + \frac{MR.NR.\alpha y(T_1).\cos(\psi)}{2} - \frac{MI.NR.\alpha y(T_1).\sin(\psi)}{2} + \frac{MR.NI.\alpha y(T_1).\sin(\psi)}{2},$$

Adopting the Routh-Hurwitz criteria, the nonlinear fixed point solution of $\alpha y(T_1)$ is stable only if:

$$C1 > 0 \text{ and } C2 > 0. \quad (42)$$

3.3. Bifurcation Analysis

Using the stationary solution assumption $\alpha(y)' = \psi' = 0$
To eliminate $\cos(\psi)$ and $\sin(\psi)$ from the Jacobian in Equation (39), thus:

$$J = \begin{bmatrix} -\frac{NR.\alpha y(T_1)}{2} & -\frac{NI.\alpha y(T_1)^2}{4} - \frac{\sigma_2}{2} \\ -\frac{NI.\alpha y(T_1)}{2} & \frac{NR.\alpha y(T_1)^2}{4} \end{bmatrix}, \quad (43)$$

The characteristics equation is obtained by solving for the Eigenvalues of the Jacobian,

$$|J - \vartheta I| = 0, \text{where } \vartheta \text{ are the Eigenvalues.}$$

$$\vartheta^2 + \left(\frac{NR.\alpha y(T_1)}{2} - \frac{NR.\alpha y(T_1)^2}{4}\right)\vartheta - \left(\frac{NI^2.\alpha y(T_1)^3}{8} + \frac{NI.\alpha y(T_1).\sigma_2}{4} + \frac{NR^2.\alpha y(T_1)^3}{8}\right) = 0, \quad (44)$$

The sum of the solutions of the characteristic polynomial is $\vartheta_1 + \vartheta_2 = \frac{NR.\alpha y(T_1).(\alpha y-2)}{4}$. However, for positive values of NR and $\alpha y(T_1) < 2$, there cannot be a pure imaginary pair of eigenvalues. Hence, Hopf bifurcations cannot exist for the system. However, the possibilities of having a simple zero eigenvalue cannot be ruled out, the likely bifurcations are saddle-node, pitchfork and transcritical bifurcations. Thus by setting $\vartheta = 0$ in the characteristic polynomial (44), it is observed that such bifurcations require the following conditions to be satisfied:

$$\alpha y(T_1) = 0 \text{ or } \alpha y(T_1)^2 = \frac{-2.NI.\sigma_2}{NI^2+NR^2} \quad (45)$$

The value of $\alpha y(T_1)$ needs to satisfy Equation (35). With σ_2 as the controlling parameter, the frequency response curve is expected to bifurcate at three points; namely A, B and C.

$$(\sigma_2, 0)_{1,2} = \left(2\sqrt{MI^2 + MR^2}, 0\right), \left(-2\sqrt{MI^2 + MR^2}, 0\right)$$

$$(\sigma_2, \alpha y(T_1)) = \frac{-2\sqrt{\frac{MI^2+MR^2}{NI^2+NR^2}}(NI^2+NR^2)}{NR} \text{ (Softening) and}$$

$$(\sigma_2, \alpha y(T_1)) = \frac{2\sqrt{\frac{MI^2+MR^2}{NI^2+NR^2}}(NI^2+NR^2)}{NR} \text{ (Hardening)} \quad (46)$$

To ascertain the possibility of only having saddle node and pitchfork bifurcations, vertical tangency of the equilibrium curves can be checked. Rearranging and squaring the second solution presented in Equation (35) gives;

$$((NI^2 + NR^2)\alpha y(T1)^2 + 2.NI.\sigma_2)^2 = \left(2\sqrt{4.MI^2.NI^2 + 4.MI^2.NR^2 + 4.MR^2.NI^2 + 4.MR^2.NR^2 - NR^2{\sigma_2}^2}\right)^2 \quad (47)$$

Differentiating both side with respect to $\alpha y(T_1)$:

$$2((NI^2 + NR^2)\alpha y(T_1)^2 + 2.NI.\sigma_2)\left(2(NI^2 + NR^2)\alpha y(T_1)^2 + 2.NI.\frac{d\sigma_2}{d\alpha y}\right) = 16NR^2{\sigma_2}^2\sigma_2\frac{d\sigma_2}{d\alpha y} \quad (48)$$

Vertical tangency of the curve $\alpha y(T_1) = \alpha y(T_1)(\sigma_2)$ demands that; $\frac{d\alpha y(T_1)}{d\sigma_2} \to \infty$, Therefore, $\frac{d\sigma_2}{d\alpha y(T_1)} \to 0$. Substituting $\frac{d\sigma_2}{d\alpha y(T_1)} = 0$ in Equation (48), it is seen that vertical tangency occurs at:

$$\alpha y(T_1) = 0 \text{ or } \alpha y(T_1)^2 = \frac{-2.NI.\sigma_2}{NI^2+NR^2} \quad (49)$$

The bifurcation points are obtained at A, B and C. Again, this confirmed the presence of one saddle-node and two pitchfork bifurcations.

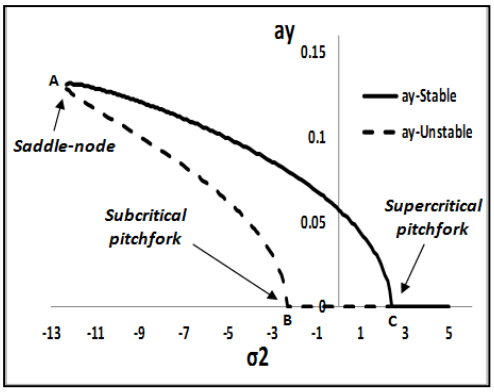

Figure 2: Typical Frequency response curves with bifurcation points.

At equilibrium, it's identified as detailed in Equations (43-49) that point A is a saddle-node bifurcation and points B and C are subcritical and supercritical pitchfork bifurcations respectively. According to Thomsen, (2003); the distinction between subcritical and supercritical bifurcations is not tied to the nature of the branches, but to their stability. For a supercritical bifurcation, a

stable solution becomes unstable, and two stable branches come out on each side of the unstable solutions. On the other hand, for subcritical bifurcation an unstable solution achieves stability, and two branches of unstable solutions emerged. However, for periodic solutions, the saddle node at point A also corresponds to cyclic-fold bifurcation while the subcritical pitchfork bifurcation and supercritical pitchfork bifurcations at B and C also corresponds to subcritical and super critical Hopf bifurcations respectively (Thomsen, 2003, Nayfeh and Balachandran, 2004).

4. RESULTS AND DISCUSSION

This section presents the numerical solutions of the nonlinear dynamics of a cantilever pipe, conveying steady pressurized air/water two-phase flow. The transverse linear natural frequencies are estimated by solving Equations (19) and (20) simultaneously with a numeric code written in Matlab.

Table 1: Summary of pipe and flow parameter

Parameter Name	Parameter Unit	Parameter Values
External Diameter	D_o (m)	0.0113772
Internal Diameter	D_i (m)	0.00925
Length	L (m)	0.1467
Pipe density	ρ_{pipe} (kg/m^3)	7800
Young's Modulus	E (N/m^2)	207E11
Gas density	ρ_{Gas} (kg/m^3)	1.225
Water density	ρ_{Water} (kg/m^3)	1000

In the manner of [7], the Argand diagram of the Eigen-frequencies is used to find the critical velocities of the two-phase flow for the various void fractions (0.1, 0.3 and 0.5). The critical velocities for the two phase flow is obtained and presented in Table 2.

Table 2: Summary of the linear two-phase solution of critical flow velocities

Fluid	Void Fraction	β Liquid	β Gas	Ψ Liquid	Ψ Gas	Critical mixture velocity	
						Transverse	Axial
Two-phase	0.1	0.19999	0.00003	0.99986	0.00014	11.502	29.004
Two-phase	0.3	0.19998	0.00010	0.99948	0.00052	12.505	31.634
Two-phase	0.5	0.19995	0.00024	0.99878	0.00122	14.613	36.966

* Critical mixture velocity based on Hopf bifurcation of 2nd mode

In the absence of internal resonance, the near resonant frequency response of the transverse vibrations is shown by [9] as a similitude of Duffing equation with parametric excitation or of nonlinear Mathieu's equation. The response peaks tilts over to the left, indicating nonlinear restoring forces of the softening type. However, the work shows that for amplitudes of pulsation of phases taken as μ_1= 0.1, and μ_2=0.2 at a post critical velocity of 16, the frequency response curves transit between subcritical and supercritical bifurcation as the void fraction increases from 0.1 to 0.3. To track the transition, bifurcation points on the frequency response curve was initially identified by Equations (43-49), and their variations examined with changes in the void fractions of the two phase flow.

The plots show the near resonant frequency response curve for the transverse vibrations of pipe that conveys pulsating gas-liquid two phase flow at mixture flow velocity of 16 for various void fractions. The system exhibits a softening non-linear restoring force with the peak tilting to the left. Consequently, jumps and multiple solutions exist at some values of the detuning parameter. As seen from the plots, the dynamics changed qualitatively at points A, B and C. Assessing the similarity between the analytical values and the bifurcations points from the plot of the numerical solution obtained by solving Equation 34 using the MATLAB's "solve" nonlinear routine, it can be seen that a good comparison is obtained.

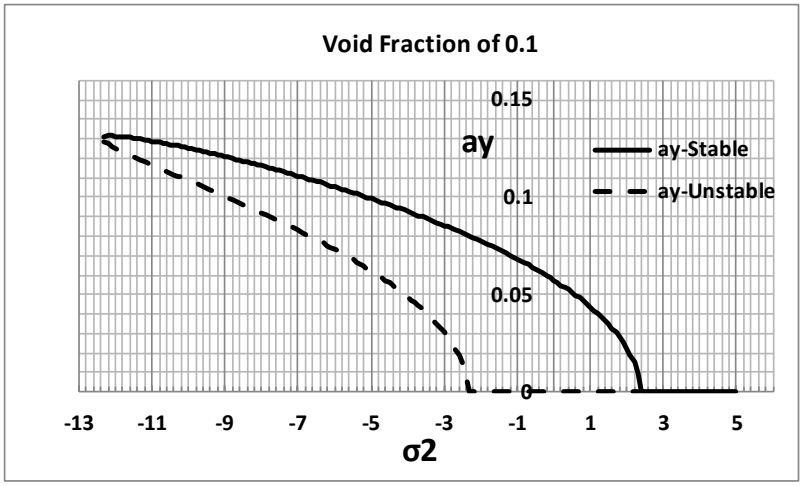

Figure 3: Frequency response curve with bifurcation points for void fraction of 0.1.

Table 3: Analytical results of the bifucation points for void fraction of 0.1

Saddle Node bifurcation point A	Pitchfork bifurcation points B and C	
$\frac{-2\sqrt{\frac{MI^2+MR^2}{NI^2+NR^2}}(NI^2+NR^2)}{NR}$	$-2\sqrt{MI^2+MR^2}$	$2\sqrt{MI^2+MR^2}$
-12.3634	-2.3387	2.3387

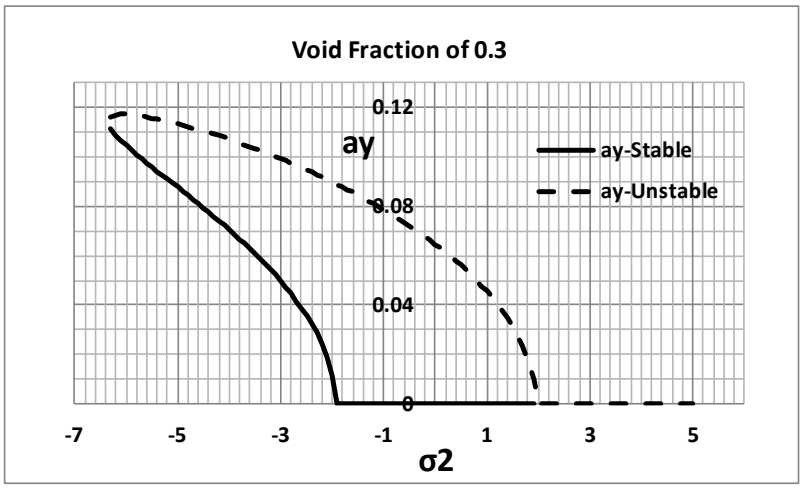

Figure 4: Frequency response curve with bifurcation points for void fraction of 0.3.

Table 4: Analytical results of the bifucation points for void fraction of 0.3

Saddle Node bifurcation point A	Pitchfork bifurcation points B and C	
$\frac{-2\sqrt{\frac{MI^2+MR^2}{NI^2+NR^2}}(NI^2+NR^2)}{NR}$	$-2\sqrt{MI^2+MR^2}$	$2\sqrt{MI^2+MR^2}$
-6.3647	-1.9227	1.9227

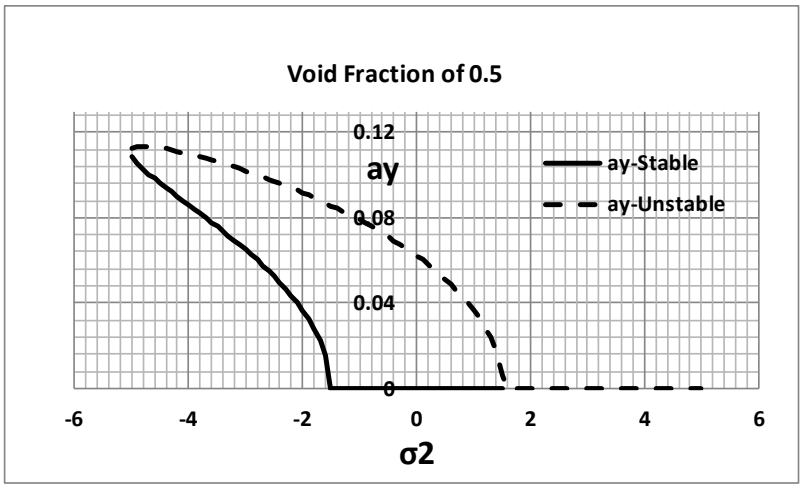

Figure 5: Frequency response curve with bifurcation points for void fraction of 0.5.

Table 5: Analytical results of the bifucation points for void fraction of 0.5

Saddle Node bifurcation point A	Pitchfork bifurcation points B and C	
$\frac{-2\sqrt{\frac{MI^2+MR^2}{NI^2+NR^2}}(NI^2+NR^2)}{NR}$	$-2\sqrt{MI^2+MR^2}$	$2\sqrt{MI^2+MR^2}$
-5.0295	-1.5010	1.5010

Table 6: Comparison between analytical and numerical results

Void fraction	Points	Analytical	Numerical	Percentage error (%)
0.1	**A**	-12.3634	-12.3	0.51
	B	-2.3387	-2.3	1.65
	C	2.3387	2.3	1.65
0.3	**A**	-6.3647	-6.3	1.02
	B	-1.9227	-1.9	1.18
	C	1.9227	1.9	1.18
0.5	**A**	-5.0295	-5	0.59
	B	-1.5010	-1.5	0.07
	C	1.5010	1.5	0.07

4.1. Effect of void fraction on the bifurcation points

To investigate the transition between subcritical pitchfork bifurcation and supercritical pitchfork bifurcations at point B and C as the void fraction changes from 0.1 to 0.3 for a mixture velocity of 16, various void fraction between 0.1 and 0.3 were examined for a range of detuning

parameter between ± 3. Figure 6 shows a plot of the amplitudes as a function of the void fraction and detuning parameter; Figure 6(a and b) corresponds to the occurrence at point B and C respectively. Results show that the transition occurred between void fractions of 0.2 and 0.21.

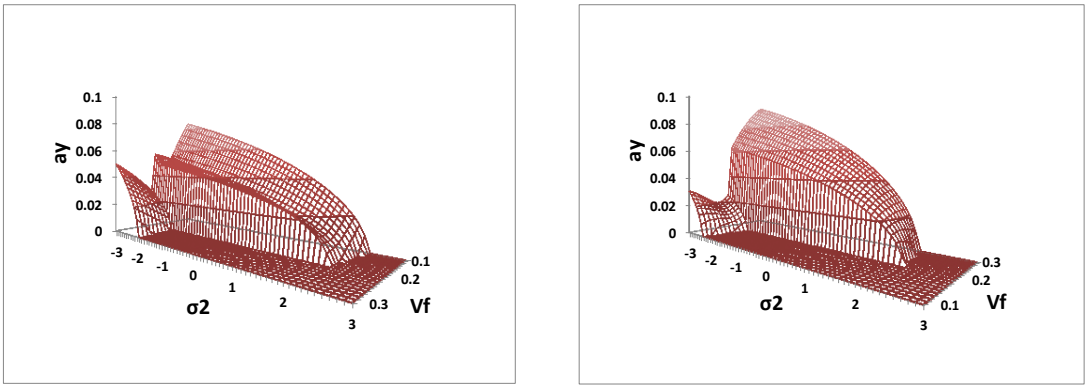

(a) (b)

Figure 6: Frequency response curves for various void fractions between 0.1 and 0.3 in the detuned range $-3 < \sigma_2 < 3$; (a) At point B, (b) At point C.

With the transition point narrowed down, frequency response curves are presented in Figure 7 for void fractions 0.2 to 0.21 with a step size of 0.0025. The plots show that the transition actually occurred between void fractions of 0.2025 and 0.205.

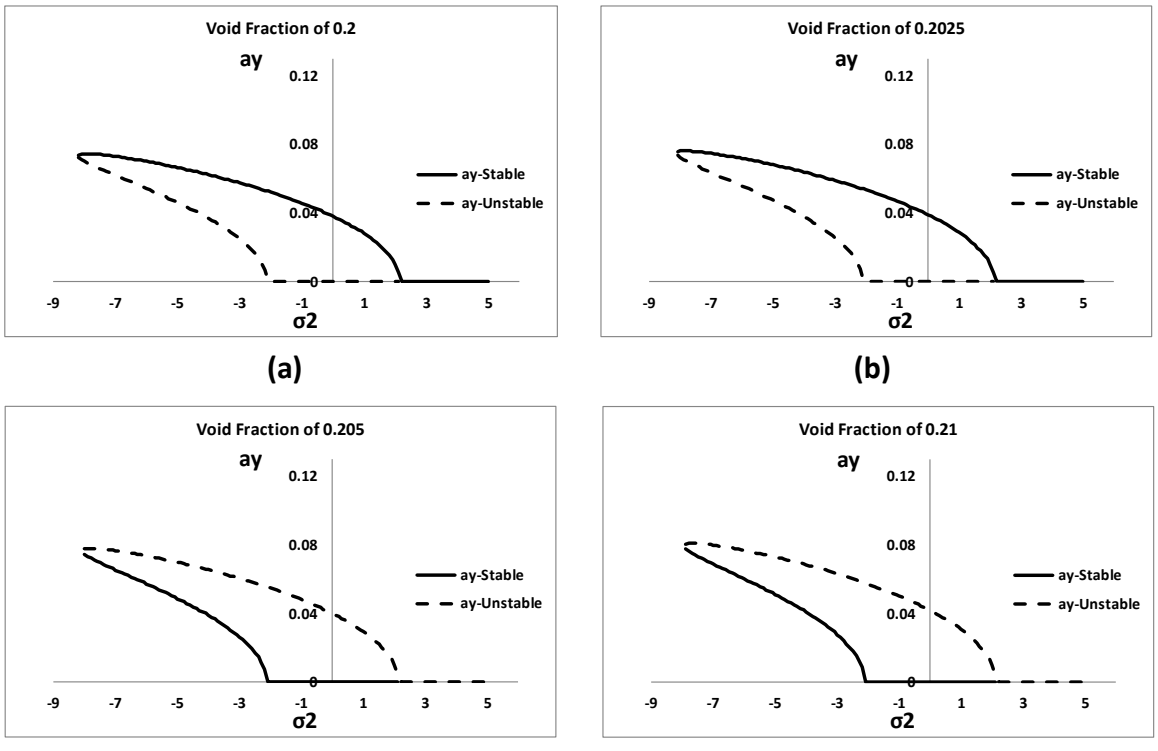

(a) (b)

(c) (d)

Figure 7: Frequency response curves for various void fractions between 0.2 and 0.21

4. CONCLUSION

This work uses the method of multiple scale perturbation to analyze the stability and pitchfork bifurcation of the transverse vibration of a cantilevered pipe conveying pulsating two phase flow.

The system presents 1:2 parametric relationship as observed between the pulsating frequencies and the frequency of transverse vibration. The response of the pipe is characterizes by a nonlinear softening behavior with the presence of jumps and multiple solutions. Analytical bifurcation assessment shows that the system exhibits a saddle node bifurcation and subcritical pitchfork and supercritical pitchfork bifurcations; this validates the outcome of the numerical simulations. The two pitchfork bifurcation points for the trivial solutions are observed to transit between supercritical pitchfork bifurcation and subcritical pitchfork bifurcation at a void fraction when the mixture flow velocity is higher than the critical mixture velocity.

Appendix

$$B1 = \left(C21\frac{\partial\eta(x)}{\partial x}\overline{U}_1 + C22\frac{\partial\eta(x)}{\partial x}\overline{U}_2 + 2\eta(x)\lambda i\right)$$

$$B2 = 6\left(\frac{\partial\eta(x)}{\partial x}\right)^2\frac{\partial\overline{\eta(x)}}{\partial x} + 2\left(\frac{\partial\eta(x)}{\partial x}\right)^2\frac{\partial^4\overline{\eta(x)}}{\partial x^4} + 4\frac{\partial\eta(x)}{\partial x}\frac{\partial\overline{\eta(x)}}{\partial x}\frac{\partial^4\eta(x)}{\partial x^4} + 8\frac{\partial\eta(x)}{\partial x}\frac{\partial^2\overline{\eta(x)}}{\partial x^2}\frac{\partial^3\eta(x)}{\partial x^3} +$$

$$8Y(T_1)^2\overline{Y(T_1)}\frac{\partial\overline{\eta(x)}}{\partial x}\frac{\partial^2\eta(x)}{\partial x^2}\frac{\partial^3\eta(x)}{\partial x^3} - 3C6\frac{\partial\eta(x)}{\partial x}\frac{\partial\overline{\eta(x)}}{\partial x}\frac{\partial^2\eta(x)}{\partial x^2} + 8\frac{\partial\eta(x)}{\partial x}\frac{\partial^2\eta(x)}{\partial x^2}\frac{\partial^3\overline{\eta(x)}}{\partial x^3} - \frac{3}{2}C6\left(\frac{\partial\eta(x)}{\partial x}\right)^2\frac{\partial^2\eta(x)}{\partial x^2}$$

$$B3 = \left(\frac{1}{2}\left(C22\mu_2\frac{\partial\eta(x)}{\partial x}\overline{U}_2\lambda\right) - \frac{1}{2}\left(C42\Omega_2\mu_2\frac{\partial\eta(x)}{\partial x}\overline{U}_2\right) + aC32\mu_2\frac{\partial^2\eta(x)}{\partial x^2}\overline{U}_2{}^2 i - C32\mu_2\frac{\partial^2\eta(x)}{\partial x^2}\overline{U}_2{}^2 i\right)$$

$$B4 = \left(\frac{1}{2}\left(C21\mu_1\frac{\partial\eta(x)}{\partial x}\overline{U}_1\lambda\right) - \frac{1}{2}\left(C41\Omega_1\mu_1\frac{\partial\eta(x)}{\partial x}\overline{U}_1\right) + aC31\mu_1\frac{\partial^2\eta(x)}{\partial x^2}\overline{U}_1{}^2 i - C31\mu_1\frac{\partial^2\eta(x)}{\partial x^2}\overline{U}_1{}^2 i\right)$$

$$B5 = \left(\frac{1}{2}\left(C22\mu_2\frac{\partial\overline{\eta(x)}}{\partial x}\overline{U}_2\lambda\right) - \frac{1}{2}\left(C42\Omega_2\mu_2\frac{\partial\overline{\eta(x)}}{\partial x}\overline{U}_2\right) + aC32\mu_2\frac{\partial^2\overline{\eta(x)}}{\partial x^2}\overline{U}_2{}^2 i - C32\mu_2\frac{\partial^2\overline{\eta(x)}}{\partial x^2}\overline{U}_2{}^2 i\right)$$

$$B6 = \left(\frac{1}{2}\left(C21\mu_1\frac{\partial\overline{\eta(x)}}{\partial x}\overline{U}_1\lambda\right) - \frac{1}{2}\left(C41\Omega_1\mu_1\frac{\partial\overline{\eta(x)}}{\partial x}\overline{U}_1\right) + aC31\mu_1\frac{\partial^2\overline{\eta(x)}}{\partial x^2}\overline{U}_1{}^2 i - C31\mu_1\frac{\partial^2\overline{\eta(x)}}{\partial x^2}\overline{U}_1{}^2 i\right)$$

$$B7 = \left(\frac{1}{2}\left(C22\mu_2\frac{\partial\overline{\eta(x)}}{\partial x}\overline{U}_2\lambda\right) - \frac{1}{2}\left(C42\varepsilon\sigma_2\mu_2\frac{\partial\overline{\eta(x)}}{\partial x}\overline{U}_2\right) + aC32\mu_2\frac{\partial^2\overline{\eta(x)}}{\partial x^2}\overline{U}_2{}^2 i - C32\mu_2\frac{\partial^2\overline{\eta(x)}}{\partial x^2}\overline{U}_2{}^2 i\right)$$

$$B8 = \left(\frac{1}{2}\left(C21\mu_1\frac{\partial\overline{\eta(x)}}{\partial x}\overline{U}_1\lambda\right) - \frac{1}{2}\left(C41\varepsilon\sigma_2\mu_1\frac{\partial\overline{\eta(x)}}{\partial x}\overline{U}_1\right) + aC31\mu_1\frac{\partial^2\overline{\eta(x)}}{\partial x^2}\overline{U}_1{}^2 i - C31\mu_1\frac{\partial^2\overline{\eta(x)}}{\partial x^2}\overline{U}_1{}^2 i\right)$$

ACKNOWLEDGEMENT

We gratefully thank the Petroleum Technology Development Fund (PTDF) of Nigeria for financing this study.

REFERENCES

Gregory, R.W. and Païdoussis, M.P. (1966), "Unstable Oscillation of Tubular Cantilevers Conveying Fluid. I. Theory", Proceedings of the Royal Society of London. Series A. Mathematical and Physical Sciences Vol. 293, pp.512–527.

Païdoussis, M.P. and Issid, N.T. (1974), "Dynamic Stability of Pipes Conveying Fluid", Journal of Sound and Vibration, Vol. 33(3), pp. 267–294.

Shilling, R. and Lou, Y. K. (1980), "An Experimental Study on the Dynamic Response of a Vertical Cantilever Pipe Conveying Fluid" Journal of Energy Resource Technology, Vol. 102(3), pp. 129–135.

Semler, C., Li, G.X. and Païdoussis, M.P. (1994), "The Nonlinear Equations of Motion of Pipes Conveying Fluid" Journal of Sound and Vibration, Vol. 169, pp. 577–599.

Ghayesh, M.H., Païdoussis, M.P. and Amabili, M. (2013), "Nonlinear Dynamics of Cantilevered Extensible Pipes Conveying Fluid" Journal of Sound and Vibration, Vol. 332, pp. 6405–6418.

Monette, C. and Pettigrew, M.J. (2004), "Fluidelastic Instability of Flexible Tubes Subjected to Two –phase Internal Flow" Journal of Fluids and Structures, Vol. 19, pp. 943–956.

Adegoke, A. S. and Oyediran, A. A. (2018), "Natural Frequencies, Modes and Critical Velocities of Top Tensioned Cantilever Pipes Conveying Pressurized Steady Two-phase Flow Under Thermal Loading" Research on Engineering Structures and Materials, Vol. pp. 4 297-323.

Adegoke, A. S. and Oyediran, A. A. (2017), "The Analysis of Nonlinear Vibrations of Top-Tensioned Cantilever Pipes Conveying Pressurized Steady Two-Phase Flow under Thermal Loading". Mathematical and Computational Applications, Vol. 22: 44.

Adegoke, A. S., Fashanu, T.A. and Oyediran, A. A. (2019), "Nonlinear Coupled Axial and Transverse Vibrations of a Cantilevered Pipe Conveying Pulsating Two Phase Flow". First International Nonlinear Dynamics

Conference Book of Abstract ISBN 978-88-944229-0-0 pp. 421-422

Wang, L., Yang, Y., Li, Y. and Wang, Y. (2018), "Dynamic Behaviours of Horizontal gas-Liquid Pipes Subjected to Hydrodynamic Slug Flow: Modelling and experiments" International Journal of Pressure Vessels and Pipping, Vol. 161, pp. 50-57.

An, C., and Su, J. (2015), "Dynamic Behavior of Pipes Conveying Gas-Liquid Phase Flow" Nuclear Engineering and Design, Vol. 292, pp. 204-212.

Woldesemayat, M.A. and Ghajar, A.J. (2007), "Comparison of Void Fraction Correlations for Different Flow Patterns in Horizontal and Upward Inclined Pipes" International Journal of Multiphase Flow, Vol.33, pp. 347–370.

Nayfeh, A.H. (2004), "Perturbation Methods" Wiley-VCH Verlag GmbH & Co. KGaA, Weinheim, ISBN 9780471399179.

Nayfeh, A.H. and Mook, D.T. (1995), "Nonlinear Oscillations" John Wiley and sons, Inc. ISBN 0471121428.

Thomsen, J.J. (2003), "Vibrations and Stability" Springer, ISBN 3540401407.

Nayfeh, A.H. and Balachandran, B. (2004), "Applied Nonlinear Dynamics" Wiley-VCH Verlag GmbH & Co. KGaA, Weinheim, ISBN 9780471593485.